High virulence does not necessarily impede viral adaptation to a new host: A case study using a plant RNA virus

Anouk Willemsen[1], Mark P. Zwart[1,2], Santiago F. Elena[1,3]

[1]Instituto de Biología Molecular y Celular de Plantas (IBMCP), Consejo Superior de Investigaciones Científicas-Universidad Politécnica de Valencia, Campus UPV CPI 8E, Ingeniero Fausto Elio s/n, 46022 València, Spain.

[2]Institute of Theoretical Physics, University of Cologne, Zülpicher Straße 77, 50937 Cologne, Germany.

[3]The Santa Fe Institute, 1399 Hyde Park Road, Santa Fe, NM 87501, USA.

E-mail addresses: anwil1@ibmcp.upv.es (AW), mark.zwart@wur.nl (MPZ), sfelena@ibmcp.upv.es (SFE).

Corresponding author: AW (anwil1@ibmcp.upv.es)

Abstract

Background: When between-host selection pressures predominate, theory suggests that high virulence could hinder between-host transmission of microparasites, and that virulence therefore will evolve to lower levels that optimize between-host transmission. Highly virulent microparasites could also curtail host development, thereby limiting both the host resources available to them and their own within-host effective population size. High virulence might therefore curtail the mutation supply rate and increase the strength with which genetic drift acts on microparasite populations, thereby limiting the potential to adapt to the host and ultimately perhaps the ability to evolve lower virulence. As a first exploration of this hypothesis, we evolved *Tobacco etch virus* carrying an eGFP fluorescent marker in two semi-permissive host species, *Nicotiana benthamiana* and *Datura stramonium*, for which it has a large difference in virulence. We compared the results to those previously obtained in the typical host, *Nicotiana tabacum*, where we have shown that carriage of *eGFP* has a high fitness cost and its loss serves as a real-time indicator of adaptation.

Results: After over half a year of evolution, we sequenced the genomes of the evolved lineages and measured their fitness. During the evolution experiment, marker loss leading to viable virus variants was only observed in one lineage of the host for which the virus has low virulence, *D. stramonium*. This result was consistent with the observation that there was a fitness cost of *eGFP* in this host, while surprisingly no fitness cost was observed in the host for which the virus has high virulence, *N. benthamiana*. Furthermore, in both hosts we observed few lineages with increases in viral fitness, and host-specific convergent evolution at the genomic level was only found in *N. benthamiana*.

Conclusions: The results of this study do not lend support to the hypothesis that high virulence impedes microparasites' evolution. Rather, they exemplify that jumps between host species can be game changers for evolutionary dynamics. When considering the evolution of

50 genome architecture, host species jumps might play a very important role, by allowing
51 evolutionary intermediates to be competitive.
52
53 **Keywords**: Adaptation, Experimental evolution, Host-pathogen interactions, Virulence, Virus
54 evolution, Genome architecture evolution
55
56
57
58
59
60
61
62
63
64
65
66
67
68
69
70
71

Background

From both applied and fundamental perspectives, virulence is a key phenotypic trait of microparasites. In medicine and agriculture, it is crucial to understand mechanistically how microparasites harm the host, in order to devise effective interventions. From a more fundamental perspective, evolutionary biologists have long been interested in understanding why many microparasites are highly virulent. It has been suggested that virulence reduces between-host transmission, and that selection would therefore act to maximize between-host transmission by reducing virulence [1, 2]. High virulence would signal maladaptation, for example following a host-species jump, and eventually be selected against. The ubiquity of microparasitic virulence and the fact that many apparently well-adapted microparasites have high virulence led to a more sophisticated framework: the hypothesis that there are tradeoffs between virulence and transmission [2–5]. This framework posits that high levels of replication could increase the probability of a microparasite being transferred to a new host, whilst also increasing the probability that the host would die quickly and the temporal window for transmission would be very brief. Under this more plausible framework, virulence evolves to the level that optimizes between-host transmission [4, 6, 7].

The tradeoff hypothesis forms the cornerstone for theoretical frameworks considering the evolution of virulence in many different pathosystems. Many important additions to the framework have been made, for example recognizing that within-host competition and opportunism can lead to increases in virulence [8–10]. Moreover, the importance of other factors at the between-host level have been given consideration, such as self-shading [11]. Self-shading occurs when the host population is structured, and a highly virulent microparasite kills all host organisms in a subpopulation before transmission to another subpopulation can be achieved. The effects of evolution on microparasitic virulence have

96 therefore been given considerable attention, although the number of experimental studies that
97 address this issue is still rather limited, especially for viruses [12].
98 The effects of evolution on microparasite virulence have been widely considered. However,
99 virulence itself could also have profound effects on evolution, including its own evolutionary
100 dynamics [13]. This reversed causality is already apparent from the tradeoff model, under
101 which microparasites with suboptimal virulence will undergo reduced between-hosts
102 transmission. All other things equal, if a smaller number of hosts are infected effective
103 population size will be decreased, increasing the strength of genetic drift and decreasing the
104 mutation supply rate. In addition, the evolution to optimum virulence may be slow as this
105 optimum is not static and can shift towards lower virulence as the density of susceptible hosts
106 decreases [14]. Moreover, a wide range of virulence can be associated with each step of
107 evolution towards the optimum, where selection favors genotypes with higher fitness that may
108 improve transmission but not necessarily improve virulence [13]. Besides these effects of
109 virulence on evolution, it is conceivable that a similar within-host effect could also occur,
110 when virulence curtails host development and thereby limits the host resources available to
111 the microparasite. Virulence would then limit the microparasite effective population size
112 within hosts, again reducing the mutation supply and thereby slowing the rate of adaptation.
113 Interestingly, all of these mechanisms could limit the rate at which lower virulence evolves,
114 meaning that high virulence might persist longer than suggested by the simple tradeoff model
115 [13].
116 There are many reasons why high virulence in host-pathogen interactions could emerge, but
117 the most likely avenue is probably a change of host species. For example, infection of Ebola
118 virus in bats is asymptomatic, while in humans and other primates the death rate is high [15].
119 Changes in virulence have been explained by the host phylogeny, where similar levels of
120 virulence are displayed by closely related hosts and host jumps across large genetic distances

121 may result in high virulence [16]. However, if a microparasite is confronted with a new host
122 environment in which its level of virulence is altered, how does virulence affect its ability to
123 adapt to the new host?
124 Here we address this question using *Tobacco etch virus* (genus: *Potyvirus*, family:
125 *Potyviridae*), a (+)ssRNA virus that infects a wide-range of host plants, and an experimental
126 evolution approach. To consider the effect of virulence on virus adaptation, we looked for
127 two natural host species in which (*i*) there was some evidence that TEV potential for
128 adaptation would be roughly similar, and (*ii*) there was a large difference in virulence. The
129 distribution of mutational fitness effects (DMFE) of TEV has been compared in eight host
130 species, and this study concluded that there were strong virus genotype-by-host species
131 interactions [17]. For many host species distantly related to the typical host of TEV,
132 *Nicotiana tabacum*, the DMFE changed drastically; many mutations that were neutral or
133 deleterious in *N. tabacum*, became beneficial. However, for two closely related host species,
134 *Nicotiana benthamiana* and *Datura stramonium*, most mutations tested remained neutral or
135 deleterious [17], implying that the fraction of beneficial mutations in both hosts is small.
136 Moreover, virus accumulation after one week of infection is also similar for both hosts [18].
137 On the other hand, TEV infection of *N. benthamiana* will typically result in heavy stunting
138 and the death of the plant within a matter of weeks, whereas TEV infection of *D. stramonium*
139 is virtually asymptomatic. Whilst there are many similarities between TEV infection in these
140 two hosts, one key difference is host-pathogen interactions and therewith levels of viral
141 virulence brought about.
142 As a first exploration of the effects of virulence on microparasite evolution, we therefore
143 decided to evolve TEV in *N. benthamiana* and *D. stramonium*. By serially passaging each
144 independent lineage in a single plant, our study maximizes within-host selection. This setup
145 allows us to exclusively focus on effects of within-host selection, although for our model

146 system we expect to see large differences in the resulting population size and the scope of
147 virus movement within the host. Moreover, to immediately gauge whether adaptive evolution
148 might be occurring, we passaged a TEV variant expressing a marker protein (Fig. 1), the
149 enhanced GFP (eGFP). Upon long-duration passages in *N. tabacum*, this exogenous sequence
150 is quickly lost due to its strong fitness cost, and its loss is reliably indicated by a loss of eGFP
151 fluorescence [19]. According to the above hypothesis that high virulence may impair the rate
152 of microparasite evolution, we expect that adaptive evolution would occur more quickly in the
153 host species for which TEV has lower virulence, *D. stramonium*, than in the host species for
154 which it has high virulence, *N. benthamiana*. Hence, we expected that in *D. stramonium* (*i*)
155 the eGFP marker would be lost more rapidly, (*ii*) there would be more sequence-level
156 convergent evolution, and (*iii*) there would be larger increases in within-host competitive
157 fitness. However, the results clashed with these simple hypotheses, exemplifying the extent
158 to which a host species jump can be a game changer for RNA virus evolutionary dynamics.
159

160 ## Methods

161 ### Virus stocks, plants and serial passages

162 The TEV genome used to generate TEV-eGFP virus, was originally isolated from *N. tabacum*
163 plants [20]. To generate a virus stock of the ancestral TEV-eGFP, the pMTEV-eGFP plasmid
164 [21] was linearized by digestion with *Bgl*II prior to *in vitro* RNA synthesis using the
165 mMESSAGE mMACHINE® SP6 Transciption Kit (Ambion), as described in [22]. The third
166 true leaf of 4-week-old *N. tabacum* L var Xanthi *NN* plants was mechanically inoculated with
167 5 µg of transcribed RNA. All symptomatic tissue was collected 7 days post-inoculation (dpi).
168 For the serial passage experiments, 500 mg homogenized stock tissue was ground into fine
169 powder and diluted in 500 µl phosphate buffer (50 mM KH_2PO_4, pH 7.0, 3% polyethylene
170 glycol 6000). From this mixture, 20 µl were then mechanically inoculated on the sixth true

171 leaf of 4-week old *N. benthamiana* Domin plants and on the third true leaf of 4-week old *D.*
172 *stramonium* L plants. Ten independent replicates were used for each host plant. Based on a
173 previous study done in *N. tabacum* [19], passages of TEV-eGFP in *D. stramonium* were done
174 every 9 weeks. In *N. benthamiana* the virus induces host mortality, and therefore the
175 passages had to be restricted to 6 weeks for this host. At the end of the designated passage
176 duration all leaves above the inoculated one were collected and stored at −80 ºC. For
177 subsequent passages the frozen tissue was homogenized and a sample was ground and
178 resuspended with an equal amount of phosphate buffer [19]. Then, new plants were
179 mechanically inoculated as described above. Three passages were performed for lineages
180 evolved in *D. stramonium* and five passages for lineages evolving in *N. benthamiana*, making
181 the number of generations of evolution similar in both hosts. All plants were kept in a
182 biosafety level 2 greenhouse at 24º C with 16 h light:8 h dark photoperiod.
183
184 **Reverse transcription polymerase chain reaction (RT-PCR)**
185 To determine whether deletions occurred at the *eGFP* locus, RNA was extracted from 100 mg
186 homogenized infected tissue using the InviTrap Spin Plant RNA Mini Kit (Stratec Molecular).
187 Reverse transcription (RT) was performed using M-MuLV reverse transcriptase (Thermo
188 Scientific) and reverse primer 5'-CGCACTACATAGGAGAATTAG-3' located in the 3'UTR
189 of the TEV genome. PCR was then performed with Taq DNA polymerase (Roche) and
190 primers flanking the *eGFP* gene: forward 5'-GCAATCAAGCATTCTACTTC-3', and reverse
191 5'-CCTGATATGTTTCCTGATAAC-3'. PCR products were resolved by electrophoresis on
192 1% agarose gels.
193
194 **Virus accumulation and within-host competitive fitness assays**

Prior to performing assays, the genome equivalents per 100 mg of tissue of the ancestral virus stocks and all evolved lineages were determined for subsequent fitness assays. The InviTrap Spin Plant RNA Mini Kit (Stratec Molecular) was used to isolate total RNA of 100 mg homogenized infected tissue. Real-time quantitative RT-PCR (RT-qPCR) was performed using the One Step SYBR PrimeScript RT-PCR Kit II (Takara), in accordance with manufacturer instructions, in a StepOnePlus Real-Time PCR System (Applied Biosystems). Specific primers for the *CP* gene were used: forward 5'-TTGGTCTTGATGGCAACGTG-3' and reverse 5'-TGTGCCGTTCAGTGTCTTCCT-3'. The StepOne Software v.2.2.2 (Applied Biosystems) was used to analyze the data. The concentration of genome equivalents per 100 mg of tissue was then normalized to that of the sample with the lowest concentration, using phosphate buffer.

For the accumulation assays, 4-week-old *N. benthamiana* and *D. stramonium* plants were mechanically inoculated with 50 µl of the normalized dilutions of ground tissue. Inoculation of each viral lineage was done on the same host plant on which it had been evolved, plus TEV and the ancestral TEV-eGFP virus on each of the hosts, using three independent plant replicates per lineage. Leaf tissue was harvested 10 dpi. Total RNA was extracted from 100 mg of homogenized tissue. Virus accumulation was then determined by means of RT-qPCR for the *CP* gene of the ancestral and the evolved lineages. For each of the harvested plants, at least three technical replicates were used for RT-qPCR.

To measure within-host competitive fitness, we used TEV carrying a red fluorescent protein: TEV-mCherry as a common competitor. This virus has a similar insert size and within-host fitness compared with TEV-eGFP [19]. All ancestral and evolved viral lineages were again normalized to the sample with the lowest concentration, and 1:1 mixtures of viral genome equivalents were made with TEV-mCherry [21]. The mixture was mechanically inoculated on the same host plant on which it had been evolved, plus TEV and the ancestral TEV-eGFP

220 virus on each of the hosts, using three independent plant replicates per viral lineage. The
221 plant leaves were collected at 10 dpi, and stored at −80 ºC. Total RNA was extracted from
222 100 mg homogenized tissue. RT-qPCR for the *CP* gene was used to determine total viral
223 accumulation, and independent RT-qPCR reactions were also performed for the mCherry
224 sequence using specific primers: forward 5'-CGGCGAGTTCATCTACAAGG-3' and reverse
225 5'-TGGTCTTCTTCTGCATTACGG-3'. The ratio of the evolved and ancestral lineages to
226 TEV-mCherry (R) is then $R = (n_{CP} - n_{mCherry})/n_{mCherry}$, where n_{CP} and $n_{mCherry}$ are the
227 RT-qPCR measured copy numbers of *CP* and *mCherry*, respectively. Then we can estimate
228 the within-host competitive fitness as $W = \sqrt[t]{R_t/R_o}$, where R_0 is the ratio at the start of the
229 experiment and R_t the ratio after t days of competition [22]. The statistical analyses
230 comparing the fitness between lineages were performed using R v.3.2.2 [23] and IBM SPSS
231 Statistics version 23.
232
233 **Illumina sequencing, variants, and SNP calling**
234 For Illumina next-generation sequencing (NGS) of the evolved and ancestral lineages, the
235 viral genomes were amplified by RT-PCR using AccuScript Hi-Fi (Agilent Technologies)
236 reverse transcriptase and Phusion DNA polymerase (Thermo Scientific), with six independent
237 replicates that were pooled. Each virus was amplified using three primer sets, generating
238 three amplicons of similar size (set 1: 5'-GCAATCAAGCATTCTACTTCTATTGCAGC-3'
239 and 5'-CCTGATATGTTTCCTGATAAC-3'; set 2: 5'-ACACGTACTGGCTGTCAGCG-3'
240 and 5'-CATCAATGTCAATGGTTACAC-3'; set 3: 5'-CCCGTGAAACTCAAGATAG-3'
241 and 5'-CGCACTACATAGGAGAATTAG-3'). Equimolar mixtures of the three PCR
242 products were made. Sequencing was performed at GenoScreen (Lille, France:
243 www.genoscreen.com). Illumina HiSeq2500 2×100bp paired-end libraries with dual-index
244 adaptors were prepared along with an internal PhiX control. Libraries were prepared using

the Nextera XT DNA Library Preparation Kit (Illumina Inc.). Sequencing quality control was performed by GenoScreen, based on PhiX error rate and Q30 values.

Read artifact filtering and quality trimming (3' minimum Q28 and minimum read length of 50 bp) was done using FASTX-Toolkit v.0.0.14 [24]. De-replication of the reads and 5' quality trimming requiring a minimum of Q28 was done using PRINSEQ-lite v.0.20.4 [25]. Reads containing undefined nucleotides (N) were discarded. Initially, the ancestral TEV-eGFP sequence was mapped using Bowtie v.2.2.6 [26] against the reference TEV-eGFP sequence (GenBank accession: KC918545). Error correction was done using Polisher v2.0.8 (available for academic use from the Joint Genome Institute) and a consensus sequences was defined for the ancestral TEV-eGFP lineage. Subsequently, the cleaned reads of the evolved sequences were mapped using Bowtie v.2.2.6 against the new defined consensus sequence. Single nucleotide mutations for each viral lineage were identified using SAMtools' mpileup [27] and VarScan v.2.3.9 [28], where the maximum coverage was set to 40000 and mutations with a frequency < 1% were discarded. Note that the single nucleotide mutations detected here can be fixed (frequency > 50%) in the evolved lineages, as the detection was done over the ancestral population. Hence, it allows us to compare the mutations that arose by evolving TEV-eGFP in the different hosts.

Results

Experimental setup and fluorescent marker stability upon passaging of TEV-eGFP

TEV-eGFP was mechanically passaged in *N. benthamiana* and *D. stramonium*. In a previous study we noted that 9-week long passages led to rapid deletion of *eGFP* as well as rapid convergent evolution in *N. tabacum* [19]. Although 9-week passages could be performed in *D. stramonium*, for *N. benthamiana* this was not possible due to virus-induced host mortality. These plants died after 6 weeks of infection, and therefore we were forced to collect tissue at

this time point. As *D. stramonium* grows to similar heights as *N. tabacum* when infected with TEV, and *N. benthamiana* does not grow much after infection, we chose to maximize infection duration to make the results comparable to those obtained in *N. tabacum* [19]. We performed three 9-week passages in *D. stramonium* and – to keep the total evolutionary time comparable – five 6-week passages in *N. benthamiana*. In *D. stramonium* all ten lineages initiated were completed, whereas in *N. benthamiana* only 6/10 lineages were completed. The remaining four *N. benthamiana* lineages failed to cause infection in subsequent rounds of passaging, and were therefore halted. Initial symptomatology of TEV-eGFP in *N. benthamiana* was very mild, while this symptomatology was more severe in the second and subsequent passages, possibly indicating adaptation of the virus to this alternative host. In *D. stramonium* the symptomatology was constant along the evolution experiment.

Based on previous results, we expected that the exogenous *eGFP* gene sequence would be rapidly purged [19, 29, 30], and as such would serve as a first indicator of the occurrence of TEV adaptation. However, the usefulness of fluorescence for determining the integrity of the *eGFP* marker was limited in both hosts, by (*i*) the high levels of autofluorescence in the highly symptomatic *N. benthamiana* leaves, and (*ii*) the patchy fluorescence in the *D. stramonium* tissue. Therefore, unlike for TEV-eGFP in *N. tabacum*, the fluorescent marker was of limited use here. Nevertheless, all *N. benthamiana* lineages appeared to have some fluorescence until the end of the evolution experiment, and we observed a loss of fluorescence in only 1/10 *D. stramonium* lineages in the third 9-week passage.

After each passage, RNA was extracted from the collected leaf tissue, and RT-PCR with primers flanking the *eGFP* insert was performed. This RT-PCR assay can therefore detect deletions in the *eGFP* gene, even when deletions extend well into the downstream HC-Pro cistron [19]. In general, the RT-PCR results confirmed the fluorescence microscopy results: A large deletion was detected only in the one *D. stramonium* lineage with a loss of

295 fluorescence (Fig. 2A; 9-weeks passage 2 L8). This deletion variant went to a high frequency
296 in the subsequent passage (Fig. 2A; 9-weeks passage 3 L8). For *N. benthamiana* lineages, we
297 did detect a low-frequency deletion in the *eGFP* cistron in one lineage (Fig. 2B; 6-weeks
298 passage 4 and 5 L4), but this deletion is so large that this variant is most likely no longer
299 capable of autonomous replication. The deletion size is around 1500 nt, which means that
300 after deleting the entire *eGFP*, around 800 nt are deleted from HC-Pro, which has a size of
301 1377 nt in total. This deletion extends well into the central region of HC-Pro, beyond the
302 well-conserved FRNK box, which is essential for virus movement and RNA-silencing
303 suppressor activity [31, 32]. We performed an extra round of passaging with all *N.*
304 *benthamiana* lineages to check whether this variant would remain at a low frequency, and
305 found exactly this result (Fig. 2B; 6-week passage 6 L4). Furthermore, we detected a small
306 deletion in one lineage (Fig. 2B; 6-week passage 5 and 6 L1) that was maintained at a low
307 frequency in subsequent passages of the virus population.
308
309 **Whole-genome sequencing of the evolved lineages**
310 All evolved and the ancestral TEV-eGFP lineages were fully sequenced by Illumina
311 technology (SRA accession: SRP075180). The consensus sequence of the ancestral TEV-
312 eGFP population was used as a reference for mapping the evolved lineages. The deletion
313 observed by RT-PCR (Fig. 2A) in one of the *D. stramonium* lineages was confirmed by a low
314 number of reads mapping inside the *eGFP* region (median coverage *eGFP*: 111.5), compared
315 to a higher average coverage outside this region (median coverage *P1* gene: 19190, median
316 overall genome coverage: 18460). The large deletion included the N-terminal region of *HC-*
317 *Pro*, as observed for other deletions that occur after gene insertions before this gene [19, 34].
318 For all other lineages in *D. stramonium* and *N. benthamiana*, coverage over the genome was

largely uniform and similar to the ancestral virus population, indicating that there were indeed no genomic deletions present at appreciable frequencies.

Single nucleotide mutations were detected from a frequency as low as 1%, comparing the evolved TEV-eGFP lineages in *N. benthamiana* and *D. stramonium* to the ancestral population (Fig. 3). This detection was also performed for evolved TEV-eGFP lineages in *N. tabacum*, that were sequenced in a previous study [19] (SRA accession: SRP075228). In the evolved *N. benthamiana* lineages 165 unique mutations were found, with a median of 34.5 (range: 27 - 47) mutations per lineage. In the evolved *D. stramonium* lineages 239 unique mutations were found, with a median of 31.5 (range: 16 - 35) mutations per lineage. In the evolved *N. tabacum* lineages, 183 unique mutations were found, with a median of 21.5 (range: 17 - 36) mutations per lineage. Note that the single nucleotide mutations detected here can be fixed (frequency > 50%) in the evolved lineages, as the detection was done over the ancestral population. Hence, it allows us to compare the mutations that arose by evolving TEV-eGFP in the different hosts.

We detected only one mutation (U6286C; CI/Y2096H) that is shared between all three hosts. However, this mutation was present at a low frequency and not detected in all *D. stramonium* and *N. tabacum* lineages (Fig. 3 and Table 1). The *N. benthamiana* and *D. stramonium* lineages share more mutations (15) than either *N. benthamiana* or *D. stramonium* share with *N. tabacum* (4 and 9, respectively). However, most of these mutations are present in only a few lineages and at low frequency (Fig. 3 and Table 1).

The synonymous mutations U7092C, A7479C and A8253C, that are shared between *D. stramonium* and *N. tabacum*, are present in the highest number of lineages and reach higher frequencies comparing all shared mutations detected in the three hosts. Despite of these mutations already being present in the ancestral population, the frequencies at which these mutations are present display interesting patterns. In both *D. stramonium* and *N. tabacum* the

mutations A7479C and A8253C are always detected at the same frequency within each lineage, suggesting a strong linkage between these mutations (Additional file 1: Fig. S1). Furthermore, the U7092C mutation never appears together with the former two mutations (Additional file 1: Fig. S1), suggesting that this mutation occurs in another haplotype and that there may be sign epistasis between these two combinations of synonymous mutations. Interestingly, the ancestral U7092C, A7479C and A8253C mutations were not detected in the *N. benthamiana* lineages, demonstrating the differences in host-pathogen interactions.

Host-specific mutations were mostly found in the evolved TEV-eGFP lineages of *N. benthamiana* (Fig. 3 and Table 2). In this host, a total number of 7 specific mutations were detected, all of them being nonsynonymous. In *D. stramonium* no host-specific mutations were detected. And in *N. tabacum* only one host-specific mutation was detected in the 3'UTR (Table 2). Note that host specific mutations were defined as mutations detected in at least half of the evolved lineages. For more information on the mutations found in the three hosts please see Additional file 2: Tables S1-S3.

Viral accumulation and within-host competitive fitness

We measured virus accumulation 10 dpi, by RT-qPCR for a region within the coat protein gene (*CP*). In both host species, we found no statistically significant differences (*t*-test with Holm-Bonferroni correction) between TEV, TEV-eGFP and the lineages of TEV-eGFP evolved in that host (Fig. 4).

We then measured within-host competitive fitness by means of head-to-head competition experiments with TEV-mCherry, a virus with a different marker but similar fitness to TEV-eGFP [21]. Here we observed interesting differences between TEV and TEV-eGFP in the two different hosts. Whereas the TEV-eGFP had lower fitness than the wild-type virus in *D. stramonium* (Fig. 5, compare TEV and ancestral TEV-eGFP; *t*-test: $t_4 = 13.438$, $P < 0.001$),

there was no difference in *N. benthamiana* (Fig. 5, compare TEV and ancestral TEV-eGFP; *t*-test: $t_4 = -1.389$, $P = 0.237$). Our results therefore suggest that although there is a fitness cost associated with the *eGFP* cistron in *N. tabacum* [19] and *D. stramonium,* there is none in *N. benthamiana*. Interestingly, *N. tabacum* and *N. benthamiana* are more closely related to each other than either species is to *D. stramonium*, and yet the host species has a strong effect on the costs of a heterologous gene.

For the lineages evolved in *D. stramonium*, only for 1/10 lineages there was a significant increase in competitive fitness compared to the ancestral TEV-eGFP observed (Fig. 5, L8; *t*-test with Holm-Bonferroni correction: $t_4 = -6.890$, $P = 0.002$). This lineage is the only one to have a deletion in the *eGFP* insert. In *N. benthamiana*, 1/6 lineages had a significant increase in within-host fitness (Fig. 5, L4; *t*-test with Holm-Bonferroni correction: $t_4 = -5.349$, $P = 0.006$). However, this increase in fitness probably is not associated with the large genomic deletion for three reasons: (*i*) the wild-type TEV without the *eGFP* cistron has a similar fitness compared to the ancestral TEV-eGFP, suggesting no deletions in *eGFP* would be beneficial, (*ii*) the RT-PCR results show that this variant occurs at a low frequency in the population, and therefore is unlikely to effect strongly the results of the competition assay, and (*iii*) this deletion variant remains at low frequency during the next round of passaging (Fig. 2B), suggesting that while frequency-dependent selection might occur, its fitness is not higher than the coevolving full-length TEV-eGFP. Moreover, another lineage of *N. benthamiana* where we did not detect any deletions, also appeared to have increased in fitness (Fig. 5, L6; *t*-test: $t_4 = -4.0792$, $P = 0.015$), however, after the Holm-Bonferroni correction not significantly. Interestingly, the lineage that did increase its fitness significantly (L4) is the only lineage that contains mutations in the 6K2 protein in this host (Additional file 2: Table S1). Therefore we speculate that single-nucleotide variation is one of the main driving forces for an increase in TEV-eGFP fitness in *N. benthamiana*.

These fitness measurements show that most lineages failed to adapt to the new host species. However, in the two cases that there were significant fitness increases, the underlying genetic changes were consistent with the expected route of adaptation. In *D. stramonium*, where *eGFP* has a high fitness cost, this sequence was deleted. In *N. benthamiana*, where *eGFP* apparently has not fitness cost, host-specific single-nucleotide variation was observed.

Discussion

We set out to explore the hypothesis that differences in virulence for different hosts could have an effect on the rate of virus adaptation in each host [13]. Although we find this hypothesis simple and provocative, the observed patterns in our experiments suggest that even in a controlled laboratory environment, reality will often be complex and hard to predict. We used a virus expressing an eGFP fluorescent marker in the hope that the loss of this marker could serve as a real-time indicator of adaptation. However, there were complications with this method, and a loss of fluorescence was only observed in a single *D. stramonium* lineage. RT-PCR and Illumina sequencing confirmed the loss of the eGFP marker in this case, and its integrity in all other lineages. The data of our competitive fitness assay demonstrate why the maker sequence was probably rather stable in *N. benthamiana*; *eGFP* does not appear to have a cost in this host species, in sharp contrast to the strong fitness cost observed in *D. stramonium* as well as previously observed in the more closely related host *N. tabacum* [19]. We expect that the marker will eventually be lost, but only due to genetic drift and therefore at a slow rate.

What mechanisms might underlie the difference in the fitness costs of *eGFP* marker in these two host plants? In a previous study, we showed that the loss of the *eGFP* marker occurred more rapidly as the duration of each passage was increased [19]. During long passages transmission bottlenecks are more spaced on time, and much larger census population sizes

419 are reached. However, there is also much greater scope for virus movement into the newly
420 developing host tissues. As for *N. tabacum* [19], here we again observed that the *eGFP*
421 marker does not affect virus accumulation, whereas it does lower competitive fitness in *D.*
422 *stramonium*. These observations suggest that the effects of the *eGFP* marker on virus
423 movement are the main reason for selection against the marker. However, marker loss in *D.*
424 *stramonium* appears to occur much slower compared to *N. tabacum* [19], indicating poor
425 virus adaptation to this alternative host. Given the high virulence of TEV for *N. benthamiana*,
426 including strong stunting, there will be limited virus movement during infection and thus
427 significantly lower population census sizes. Hence, we speculate that in *N. benthamiana* the
428 limited scope for virus movement and accumulation –due to the virus' virulence itself– might
429 mitigate the cost of the *eGFP* marker. Alternatively, cell-to-cell and systemic virus
430 movement in *N. benthamiana* might be so slow that the addition of the *eGFP* marker matters
431 little. A slow systemic virus movement may also explain why in the second round of
432 infection four lineages failed to re-infect *N. benthamiana*, as initial virus accumulation
433 appeared to be very low until possible virus adaptation by means of point mutations occurred.
434 These results are at odds with our expectations, but they nevertheless have some interesting
435 implications. First, host species changes can apparently ameliorate the costs of exogenous
436 genes. Although strong virus genotype-by-host species interactions have been previously
437 shown for TEV [17], we did not anticipate that a such a simple difference (the presence of
438 *eGFP*) could also be subjected to such an interaction. These results suggest that when
439 considering the evolution of genome architecture, host species might play a very important
440 role, by allowing evolutionary intermediates to be competitive. For example, for TEV we
441 have shown that the evolution of an alternative gene order through duplication of the *NIb*
442 replicase gene is highly unlikely, as this intermediate step leads to significant decreases in
443 fitness, making the trajectory to alternative gene orders inaccessible [34]. If *NIb* duplication

has a similar interaction with host species as the *eGFP* insert has, then an alternative host species could act as a stepping-stone and hereby increase the accessibility of the evolutionary trajectory to alternative gene orders. Similar effects of environmental change have been noted in other studies [35]. The generality of these results has not been addressed yet using other viruses with altered genome architecture, but the possibilities are tantalizing. Second, our results could also have implications for assessing the biosafety risks of the genetically modified organisms. Our results suggest that extrapolating fitness results from a permissive host to alternative hosts can be problematic, even when the scope for unexpected interactions appears to be limited, as would be the case for the addition of eGFP expression. In other model systems, unexpected interactions between heterologous genes and host species have also been reported [36].

Our results were not consistent with the hypothesis that high virulence could slow down the rate of adaptation, as in each host only a single lineage had evolved higher fitness. The low rate of adaptation observed was consistent with a previous report [18], although we used passages of a longer duration here and had therefore expected more rapid adaptation [19]. Given the low rate at which lineages adapted in this experiment, however, we do not consider that our results provide strong evidence against the hypothesis. Nevertheless, our results do stress that differences in host biology can have a much stronger effect on evolutionary dynamics than differences in virus-induced virulence between host species. An alternative way to tackling the question of the effects of virulence on adaptation might be to use a biotechnological approach; hosts which have different levels of virulence can be engineered, to ensure the main difference between host treatment is microparasite-induced virulence. For example, plant hosts could be engineered to express antiviral siRNAs at low levels. Such an approach would allow for a more controlled test of the hypothesis suggested here, whilst probably not being representative for natural host populations. On the other hand, such

469 experiments could perhaps help shed light on the effects of virulence on adaptation in
470 agroecosystems or vaccinated populations.
471

472 ## Conclusions

473 A host species jump can be a game changer for evolutionary dynamics. A non-functional
474 exogenous sequence –*eGFP*– which is unstable in its typical host, has shown to be more
475 stable in two alternative host species for which TEV has both lower and higher virulence than
476 in the typical host. In addition, *eGFP* does not appear to have any fitness effects in the host
477 for which TEV has high virulence. These observations clashed with the hypothesis that high
478 virulence slows down the rate of adaptation. Moreover, when considering the evolution of
479 genome architecture, host species jumps might play a very important role, by allowing
480 evolutionary intermediates to be competitive.
481

482 ## Declarations

483 ### Ethics approval and consent to participate

484 Not applicable
485

486 ### Consent for publication

487 Not applicable
488

489 ### Availability of data and material

490 The raw read data from Illumina sequencing is available at SRA with accession: SRP075180.
491 The fitness data has been deposited on LabArchives with doi: 10.6070/H4N877TD.
492

493 ### Competing interests

494 The authors declare that they have no competing interests

495

496 **Funding**

497 This work was supported by the John Templeton Foundation [grant number 22371 to S.F.E];
498 the European Commission 7th Framework Program EvoEvo Project [grant number ICT-
499 610427 to S.F.E.]; and the Spanish Ministerio de Economía y Competitividad (MINECO)
500 [grant numbers BFU2012-30805 and BFU2015-65037-P to S.F.E]. The opinions expressed in
501 this publication are those of the authors and do not necessarily reflect the views of the John
502 Templeton Foundation. The funders had no role in study design, data collection and analysis,
503 decision to publish, or preparation of the manuscript.

504

505 **Author's contributions**

506 AW, MPZ and SFE designed the study. AW and MPZ performed the experiments. AW, MPZ
507 and SFE analyzed the data and wrote the manuscript. All authors read and approved the final
508 manuscript.

509

510 **Acknowledgements**

511 We thank Francisca de la Iglesia and Paula Agudo for excellent technical assistance.

512

513 ## Additional files

514 **Additional file 1:**

515 **Figure S1.** Frequency of mutations found in both *D. stramonium* and *N. tabacum*. Mutations
516 detected in both *D. stramonium* and *N. tabacum* that were present in all the lineages of either
517 one of these hosts. The frequency of these mutations in either the ancestral population (anc)

or the different lineages (L1-L10) is given by the color-coded points. The points are connected by the broken lines to emphasize the trend in the data.

Additional file 2:

Table S1. Mutations detected in the *Nicotiana bentiamiana* lineages as compared to the ancestral lineage

Table S2. Mutations detected in the *Datura stramonium* lineages as compared to the ancestral lineage

Table S3. Mutations detected in the *Nicotiana tabacum* lineages as compared to the ancestral lineage

References

1. Ewald PW. Host-parasite relations, vectors, and the evolution of disease severity. Annu Rev Ecol Syst. 1983;14:465–485.

2. Alizon S, Hurford A, Mideo N, Van Baalen M. Virulence evolution and the trade-off hypothesis: history, current state of affairs and the future. J Evol Biol. 2009;22:245–259.

3. Fraser C, Hollingsworth TD, Chapman R, de Wolf F, Hanage WP. Variation in HIV-1 set-point viral load: Epidemiological analysis and an evolutionary hypothesis. Proc Natl Acad Sci USA. 2007;104:17441–17446.

4. de Roode JC, Yates AJ, Altizer S. Virulence-transmission trade-offs and population divergence in virulence in a naturally occurring butterfly parasite. Proc Natl Acad Sci USA. 2008;105:7489–7494.

5. Mackinnon MJ, Gandon S, Read AF. Virulence evolution in response to vaccination: The case of malaria. Vaccine. 2008;26 Suppl 3:C42–C52.

6. Ebert D, Weisser WW. Optimal killing for obligate killers: the evolution of life histories

543 and virulence of semelparous parasites. Proc R Soc B Biol Sci. 1997;264:985–991.

544 7. Pagán I, Montes N, Milgroom MG, García-Arenal F. Vertical transmission selects for
545 reduced virulence in a plant virus and for increased resistance in the host. PLoS Pathog.
546 2014;10:e1004293.

547 8. May RM, Nowak MA. Coinfection and the evolution of parasite virulence. Proc R Soc B
548 Biol Sci. 1995;261:209–215.

549 9. de Roode JC, Pansini R, Cheesman SJ, Helinski MEH, Huijben S, Wargo AR, Bell AS,
550 Chan BHK, Walliker D, Read AF. Virulence and competitive ability in genetically diverse
551 malaria infections. Proc Natl Acad Sci. 2005;102:7624–7628.

552 10. Brown SP, Cornforth DM, Mideo N. Evolution of virulence in opportunistic pathogens:
553 generalism, plasticity, and control. Trends Microbiol. 2012;20:336–342.

554 11. Boots M, Sasaki A. The evolutionary dynamics of local infection and global reproduction
555 in host-parasite interactions. Ecol Lett. 2000;3:181–185.

556 12. Bull JJ, Lauring AS. Theory and Empiricism in Virulence Evolution. PLoS Pathog.
557 2014;10:e1004387.

558 13. Bull JJ, Ebert D. Invasion thresholds and the evolution of nonequilibrium virulence. Evol
559 Appl. 2008;1:172–182.

560 14. Lenski RE, May RM. The Evolution of Virulence in Parasites and Pathogens:
561 Reconciliation Between Two Competing Hypotheses. J Theor Biol. 1994;169:253–265.

562 15. Leroy EM, Kumulungui B, Pourrut X, Rouquet P, Hassanin A, Yaba P, Délicat A,
563 Paweska JT, Gonzalez J-P, Swanepoel R. Fruit bats as reservoirs of Ebola virus. Nature.
564 2005;438:575–576.

565 16. Longdon B, Hadfield JD, Day JP, Smith SCL, McGonigle JE, Cogni R, Cao C, Jiggins
566 FM. The Causes and Consequences of Changes in Virulence following Pathogen Host Shifts.
567 PLOS Pathog. 2015;11:e1004728.

568 17. Lalić J, Cuevas JM, Elena SF. Effect of host species on the distribution of mutational
569 fitness effects for an RNA virus. PLoS Genet. 2011;7:e1002378.
570 18. Bedhomme S, Lafforgue G, Elena SF. Multihost experimental evolution of a plant RNA
571 virus reveals local adaptation and host-specific mutations. Mol Biol Evol. 2012;29:1481–
572 1492.
573 19. Zwart MP, Willemsen A, Daròs JA, Elena SF. Experimental evolution of
574 pseudogenization and gene loss in a plant RNA virus. Mol Biol Evol. 2014;31:121–134.
575 20. Carrington JC, Haldeman R, Dolja VV, Restrepo-Hartwig MA. Internal cleavage and
576 trans-proteolytic activities of the VPg-proteinase (NIa) of tobacco etch potyvirus *in vivo*. J
577 Virol. 1993;67:6995–7000.
578 21. Zwart MP, Daròs JA, Elena SF. One is enough: in vivo effective population size is dose-
579 dependent for a plant RNA virus. PLoS Pathog. 2011;7:e1002122.
580 22. Carrasco P, Daròs JA, Agudelo-Romero P, Elena SF. A real-time RT-PCR assay for
581 quantifying the fitness of *Tobacco etch virus* in competition experiments. J Virol Methods.
582 2007;139:181–188.
583 23. R Core Team. R: A language and environment for statistical computing. 2014. Vienna,
584 Austria: R Foundation for Statistical Computing. http://www.R-project.org/. Accessed 20
585 June 2016.
586 24. FASTX-Toolkit. Hannon Lab. http://hannonlab.cshl.edu/fastx_toolkit/index.html.
587 Accessed 20 June 2016.
588 25. Schmieder R, Edwards R. Quality control and preprocessing of metagenomic datasets.
589 Bioinformatics. 2011;27:863–864.
590 26. Langmead B, Salzberg SL. Fast gapped-read alignment with Bowtie 2. Nat Methods.
591 2012;9:357–359.
592 27. Li H, Handsaker B, Wysoker A, Fennell T, Ruan J, Homer N, Marth G, Abecasis G,

593 Durbin R. The sequence alignment/map format and SAMtools. Bioinformatics.
594 2009;25:2078–2079.
595 28. Koboldt DC, Zhang Q, Larson DE, Shen D, McLellan MD, Lin L, Miller CA, Mardis ER,
596 Ding L, Wilson RK. VarScan 2: Somatic mutation and copy number alteration discovery in
597 cancer by exome sequencing. Genome Res. 2012;22:568–576.
598 29. Dolja VV, Herndon KL, Pirone TP, Carrington JC. Spontaneous mutagenesis of a plant
599 potyvirus genome after insertion of a foreign gene. J Virol. 1993;67:5968–5975.
600 30. Majer E, Daròs JA, Zwart M. Stability and fitness impact of the visually discernible
601 Rosea1 marker in the *Tobacco etch virus* genome. Viruses. 2013;5:2153–2168.
602 31. Plisson C, Drucker M, Blanc S, German-Retana S, Le Gall O, Thomas D, Bron P.
603 Structural characterization of HC-Pro, a plant virus multifunctional protein. J Biol Chem.
604 2003;278:23753–23761.
605 32. Shiboleth YM, Haronsky E, Leibman D, Arazi T, Wassenegger M, Whitham SA, Gaba V,
606 Gal-On A. The conserved FRNK box in HC-Pro, a plant viral suppressor of gene silencing, is
607 required for small RNA binding and mediates symptom development. J Virol.
608 2007;81:13135–13148.
609 33. Verchot J, Carrington JC. Debilitation of plant potyvirus infectivity by P1 proteinase-
610 inactivating mutations and restoration by second-site modifications. J Virol. 1995;69:1582–
611 1590.
612 34. Willemsen A, Zwart MP, Tromas N, Majer E, Daros JA, Elena SF. Multiple Barriers to
613 the Evolution of Alternative Gene Orders in a Positive-Strand RNA Virus. Genetics.
614 2016;202:1503–1521.
615 35. de Vos MGJ, Dawid A, Sunderlikova V, Tans SJ. Breaking evolutionary constraint with a
616 tradeoff ratchet. Proc Natl Acad Sci USA. 2015;112:14906–14911.
617 36. Hernández-Crespo P, Sait SM, Hails RS, Cory JS. Behavior of a recombinant baculovirus

618 in lepidopteran hosts with different susceptibilities. Appl Environ Microbiol. 2001;67:1140–

619 1146.

620

621 # Tables

622 **Table 1.** TEV-eGFP mutations shared in the different hosts

			N. benthamiana		*D. stramonium*		*N. tabacum*	
Nucleotide change	**Amino acid change**	**Gene**	**Number of lineages**	**Frequency range**	**Number of lineages**	**Frequency range**	**Number of lineages**	**Frequency range**
U6286C	Y2096H	CI	6/6	0.013 – 0.131	2/10	0.012 – 0.031	4/10	0.019 – 0.140
A208G	M70V	P1	1/6	0.012	1/10	0.010	-	-
C1039U	H347Y	P1	1/6	0.013	1/10	0.035	-	-
G1332A	M444I	eGFP	1/6	0.176	1/10	0.139	-	-
U1556G*	V519G	eGFP	1/6	0.011	6/10	0.010 – 0.016	-	-
U1836G	synonymous	HC-Pro	5/6	0.093 – 0.108	1/10	0.089	-	-
A1917G	synonymous	HC-Pro	1/6	0.015	1/10	0.017	-	-
A6278G	E2093G	CI	1/6	0.012	2/10	0.014 – 0.031	-	-
C6547U	H2183Y	VPg	1/6	0.013	1/10	0.014	-	-
U6747C	synonymous	VPg	1/6	0.012	1/10	0.110	-	-

A6776G	D2259G	VPg	2/6	0.533 – 0.746	1/10	0.023	-	-
G6803A	S2268N	VPg	1/6	0.014	1/10	0.024	-	-
A6438G	synonymous	6K2	1/6	0.012	1/10	0.024	-	-
C8405G*	T2802R	NIb	5/6	0.010 – 0.018	5/10	0.010 – 0.016	-	-
U9474C	synonymous	CP	1/6	0.013	1/10	0.061	-	-
C9837U	synonymous	CP	1/6	0.070	1/10	0.010	-	-
U3803C	I1268T	P3	2/6	0.656 – 0.881	-	-	2/10	0.010 – 0.019
U3872C	V2191A	P3	1/6	0.064	-	-	1/10	0.016
G4411A	V1471I	CI	1/6	0.030	-	-	1/10	0.016
C4989U	synonymous	CI	1/6	0.018	-	-	1/10	0.066
C548U	T183I	P1	-	-	1/10	0.011	1/10	0.024
G2928A*	synonymous	HC-Pro	-	-	1/10	0.017	1/10	0.999
U7092C*	synonymous	NIa-Pro	-	-	10/10	0.091 – 0.755	2/10	0.176 – 0.999
A7479C*	synonymous	NIa-Pro	-	-	10/10	0.132 – 0.790	7/10	0.960 – 0.999
A7567G	K2523E	NIa-Pro	-	-	4/10	0.012 – 0.053	10/10	0.015 – 0.871

G7710A	synonymous	NIa-Pro	-	-	1/10	0.014	1/10	0.024
A8253C*	synonymous	NIb	-	-	10/10	0.136 – 0.801	7/10	0.805 – 0.998
G9117A	synonymous	NIb	-	-	1/10	0.321	2/10	0.022 – 0.025
U9249C	synonymous	NIb	-	-	2/10	0.011 – 0.231	1/10	0.040

*Also detected in the ancestral population

623 **Table 2.** Host specific mutations in the evolved TEV-eGFP lineages.

	Nucleotide change	Amino acid change	Gene	Number of lineages	Frequency range
N. benthamiana	G3797A	G1266E	P3	3/6	0.291 – 0.664
	G4380U	E1460D	6K1	3/6	0.012 – 0.093
	U4387C	Y1463H	6K1	4/6	0.011 – 0.016
	C4391U	T1464M	6K1	6/6	0.041 – 0.138
	G4397A	S1466N	CI	6/6	0.012 – 0.019
	A6771U	L2257F	VPg	4/6	0.027 – 0.201
	G8909U*	W2970L	NIb	5/6	0.026 – 0.042
D. stramonium	-	-	-	-	-
N. tabacum	G10253A		3'UTR	10/10	0.025 – 0.040

*Also detected in the ancestral population.

624

625 ## Figure Legends

626 **Figure 1.** Schematic representation of TEV-eGFP. The *eGFP* gene is located between *P1*
627 and *HC-Pro* cistrons. Proteolytic cleavage sites were provided at both ends of *eGFP*.

628

629 **Figure 2.** Deletion detection in the *eGFP* gene. Agarose gels with RT-PCR products of the
630 region encompassing the *eGFP* gene. The TEV and TEV-eGFP are shown for comparative
631 purposes. The negative controls are healthy plants and PCR controls (C-). (A) TEV-eGFP in
632 *D. stramonium* has 10 independent lineages (L1-L10). A deletion encompassing the *eGFP*
633 gene was detected in one lineage (L8) in the second 9-week passage. This deletion went to a
634 high frequency in the subsequent passage. (B) TEV-eGFP in *N. benthamiana* has six
635 independent lineages (L1-L6). A deletion bigger than the size of *eGFP* was detected in one
636 lineage (L4) in the fourth 6-week passage. This deletion was not fixed in the two subsequent
637 passages. A small deletion was detected in the fifth and sixth 6-week passage in L1.

638

639 **Figure 3.** Genomes of the TEV-eGFP lineages evolved the three different hosts as compared
640 to the ancestral lineage. Mutations were detected using NGS data of the evolved lineages
641 (L1-L10), as compared to their ancestral population. The square symbols represent mutations
642 that are fixed (> 50%) and the circle symbols represent mutations that are not fixed (< 50%).
643 Filled symbols represent nonsynonymous substitutions and open symbols represent
644 synonymous substitutions. The triangle symbols represent mutations that are present in either
645 the 3`UTR or 5`UTR. Black substitutions occur only in one lineage, whereas color-coded
646 substitutions are repeated in two or more lineages. Note that the mutations are present at
647 different frequencies as reported by VarScan 2. Grey boxes with continuous black lines
648 indicate genomic deletions in the majority variant of the virus population. The grey
649 transparent box with dotted black lines in L4 of *N. benthamiana* indicates a genomic deletion

650 in a minority variant. The latter box was drawn to indicate the size of the deletion, assuming
651 that the deletion starts at the first position of *eGFP*. For more information on the frequency
652 of the mutations please see Additional file 2: Tables S1-S3.
653
654 **Figure 4.** Virus accumulation of the evolved and ancestral lineages. Virus accumulation, as
655 determined by accumulation experiments and RT-qPCR at 10 dpi, of TEV, the ancestral
656 TEV-eGFP, and the evolved TEV-eGFP lineages in the corresponding hosts. TEV and the
657 evolved lineage with a deletion in the *eGFP* gene are indicated with the orange bars. The
658 ancestral TEV-eGFP and the evolved lineages with an intact *eGFP* gene are indicated with
659 the green bars. Error bars represent SD of the plant replicates.
660
661 **Figure 5.** Within-host competitive fitness of the evolved and ancestral lineages. Fitness (*W*),
662 as determined by competition experiments and RT-qPCR of the different viral genotypes with
663 respect to a common competitor; TEV-mCherry. *W* was determined at 10 dpi, of TEV, the
664 ancestral TEV-eGFP, and the evolved TEV-eGFP lineages in the corresponding hosts. TEV
665 and the evolved lineage with a deletion in the *eGFP* gene are indicated with the orange bars.
666 The ancestral TEV-eGFP and the evolved lineages with an intact *eGFP* gene are indicated
667 with the green bars. The orange asterisks indicate statistical significant differences of the
668 evolved lineages as compared to TEV (*t*-test with Holm-Bonferroni correction). The green
669 asterisks indicate statistical significant differences of the evolved lineages as compared to the
670 ancestral TEV-eGFP (*t*-test with Holm-Bonferroni correction). Error bars represent SD of the
671 plant replicates.

Figure 1

TEV-eGFP

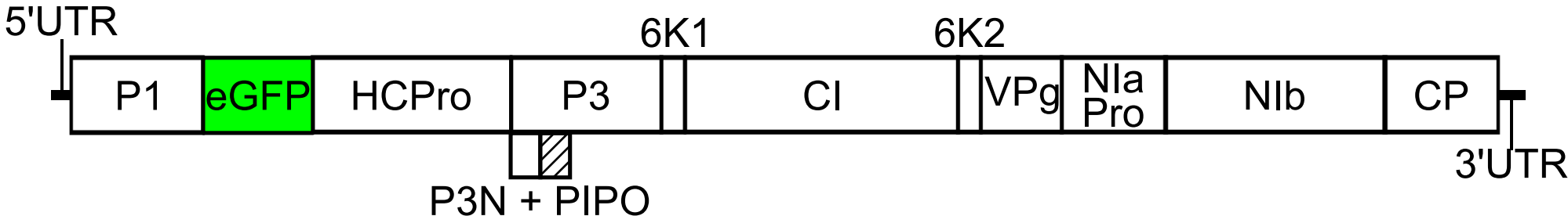

Figure 2

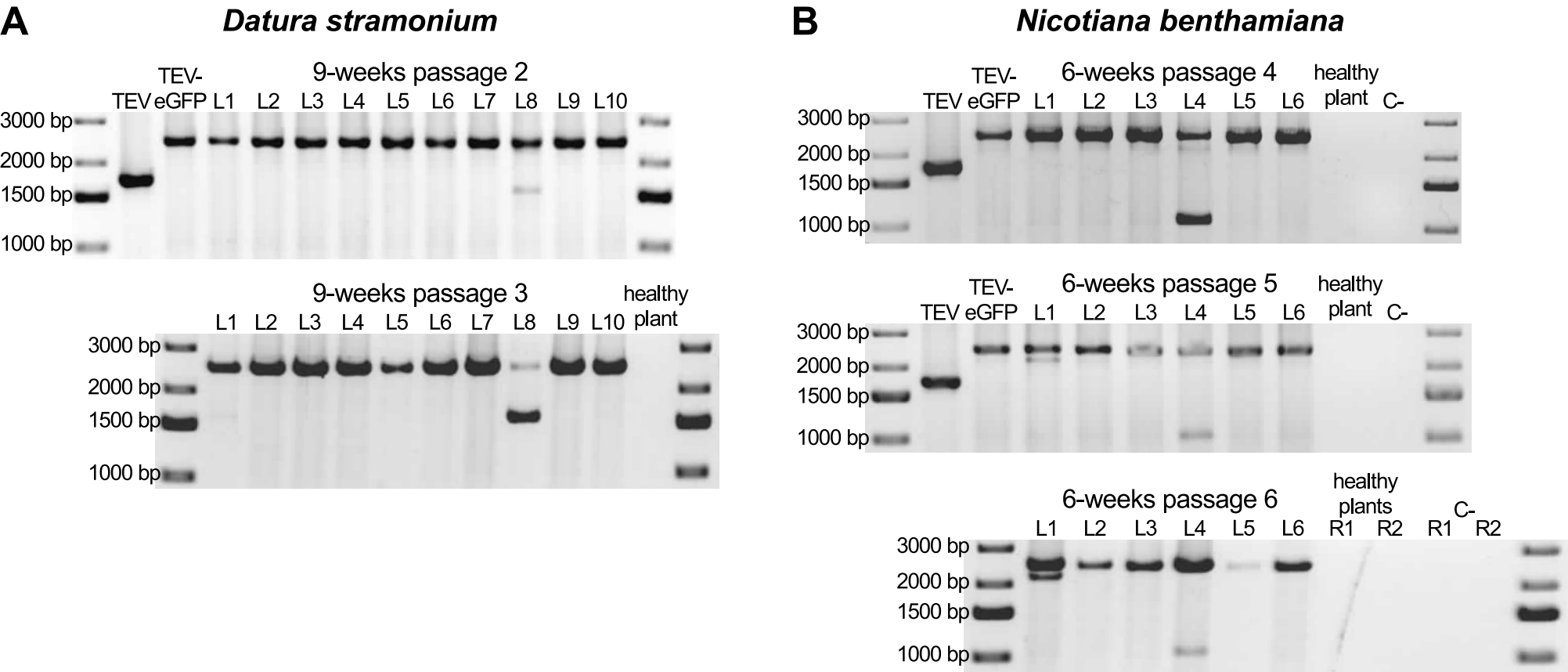
A
Datura stramonium
9-weeks passage 2
TEV
TEV-eGFP
L1
L2
L3
L4
L5
L6
L7
L8
L9
L10
3000 bp
2000 bp
1500 bp
1000 bp
9-weeks passage 3
healthy plant
B
Nicotiana benthamiana
6-weeks passage 4
C-
6-weeks passage 5
6-weeks passage 6
healthy plants
R1
R2

Figure 3

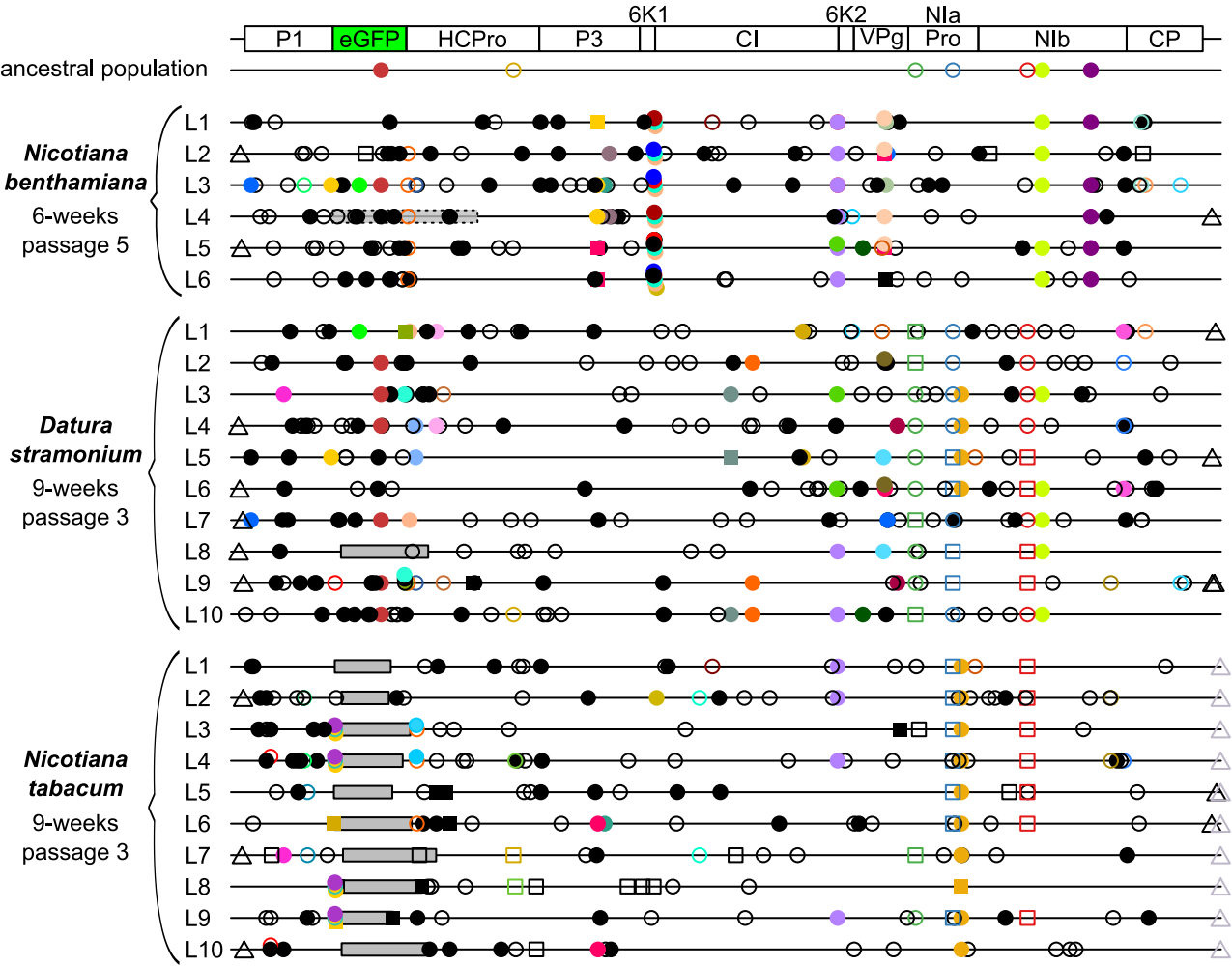
6K1
6K2
NIa
P1
eGFP
HCPro
P3
CI
VPg
Pro
NIb
CP
ancestral population
Nicotiana benthamiana
6-weeks passage 5
L1
L2
L3
L4
L5
L6
Datura stramonium
9-weeks passage 3
L1
L2
L3
L4
L5
L6
L7
L8
L9
L10
Nicotiana tabacum
9-weeks passage 3
L1
L2
L3
L4
L5
L6
L7
L8
L9
L10

Figure 4

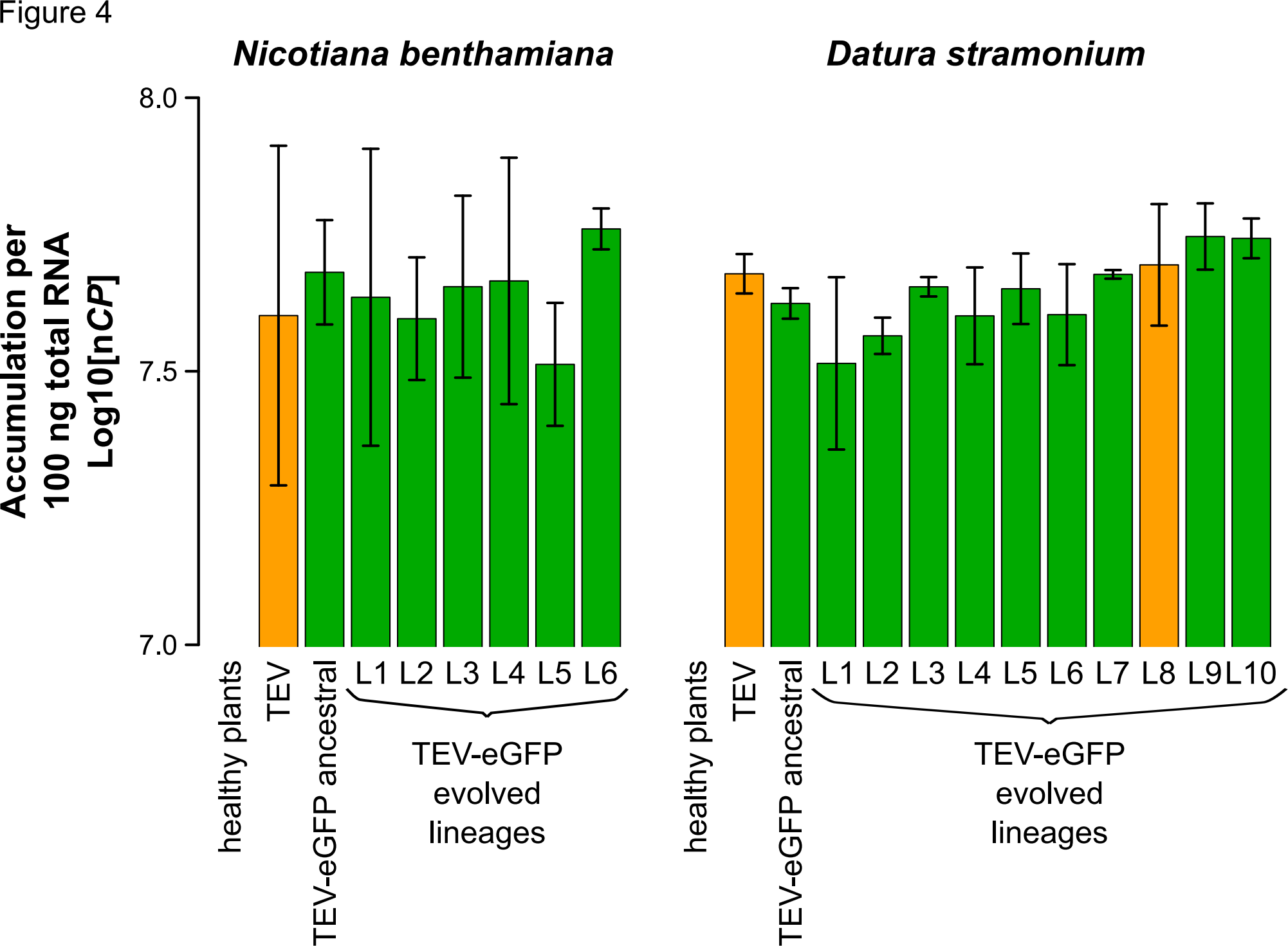
Nicotiana benthamiana
Datura stramonium
Accumulation per 100 ng total RNA Log10[nCP]
8.0
7.5
7.0
healthy plants
TEV
TEV-eGFP ancestral
L1 L2 L3 L4 L5 L6
TEV-eGFP evolved lineages
healthy plants
TEV
TEV-eGFP ancestral
L1 L2 L3 L4 L5 L6 L7 L8 L9 L10
TEV-eGFP evolved lineages

Figure 5

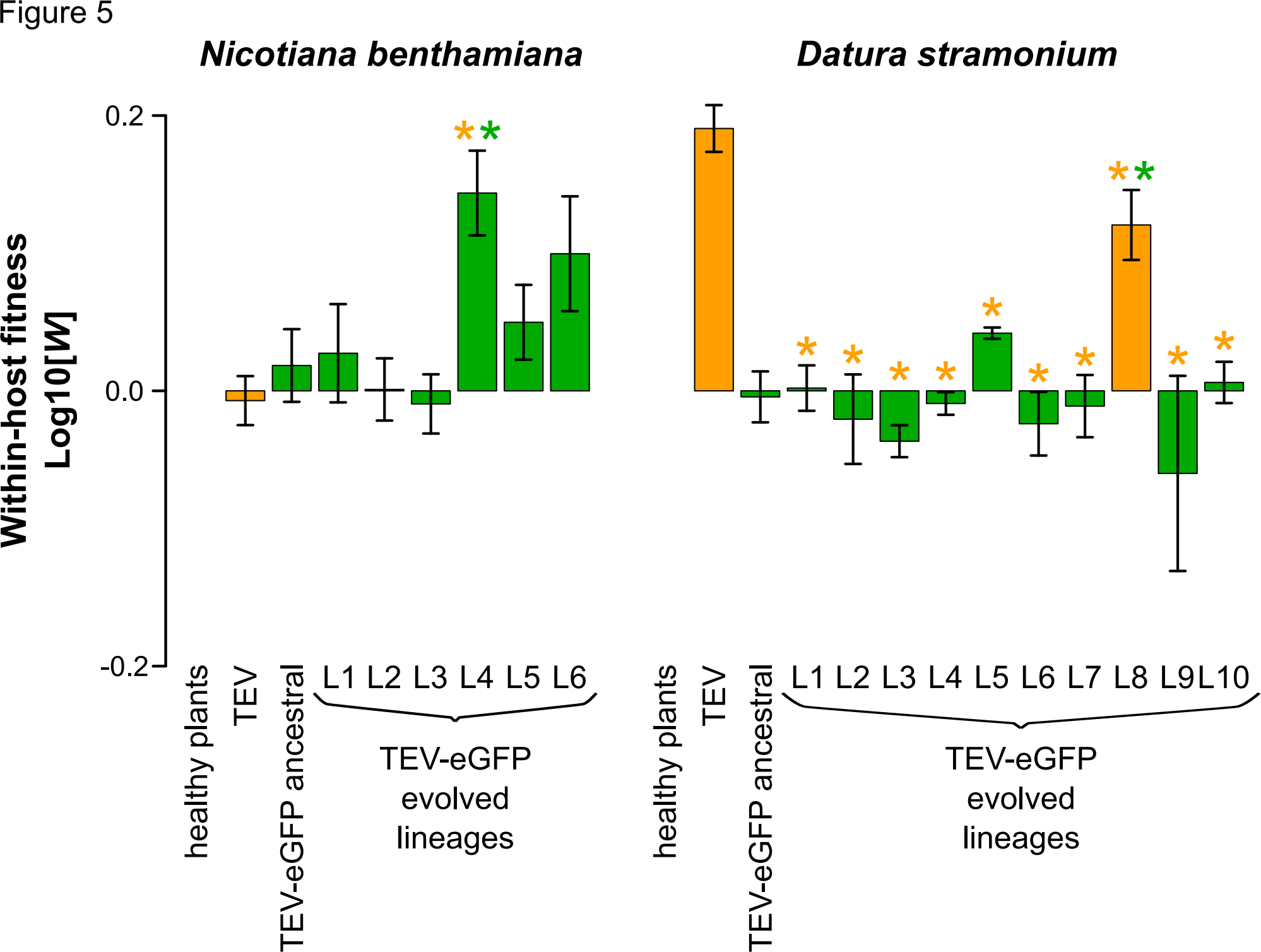
Nicotiana benthamiana
Datura stramonium
Within-host fitness
Log10[W]
0.2
0.0
-0.2
healthy plants
TEV
TEV-eGFP ancestral
L1 L2 L3 L4 L5 L6
TEV-eGFP evolved lineages
healthy plants
TEV
TEV-eGFP ancestral
L1 L2 L3 L4 L5 L6 L7 L8 L9L10
TEV-eGFP evolved lineages